European Review for Medical and Pharmacological Sciences 2018; 22: 3676-3688

miR-98-TXLNG1 (FIAT)/Sp7 function loop mediates osteoblast mineralization

L. YANG, L.-Y. HUANG, L.-B. LI, Z. TANG, K. CHEN, L.-P. CHEN, H.-Y. LUO, J. LUO, X.-L. ZHAO

Department of Endocrinology, Hunan Provincial People's Hospital, Changsha, China

Abstract. – OBJECTIVE: To investigate the role of microRNAs (miRNAs) and its mechanism in osteoblast mineralization.

MATERIALS AND METHODS: Real-time polymerase chain reaction (PCR), Northern Blot, and Western Blot were used to identify the expression mode of regulators. Overexpression and down-regulation experiments were carried out to study the role of miR-98 and interactions between regulators. Bioinformatics calculation and luciferase reporter assay were used to prove the target gene. Electrophoretic mobility shift assay (EMSA), chromatin immunoprecipitation (CHIP), and promoter luciferase reporter assay confirmed the relationship between the regulator and the promoter of miR-98.

RESULTS: MiR-98 was up-regulated during osteoblast mineralization. Overexpression of miR-98 promoted osteoblast mineralization. Factor inhibiting activating transcription factor 4 (ATF4)-mediated transcription (FIAT), a negative regulator of osteoblast differentiation, was confirmed to be a target of miR-98. As a motivator in osteoblast mineralization, Sp7 transcription factor 7 (Sp7) promoted miR-98 transcription by a combination on the promoter region.

CONCLUSIONS: Our study showed that miR-98 was an important regulator in osteoblast mineralization and miR-98 carried out its function through a novel miR-98-FIAT/Sp7 regulatory loop. It provides new insights into the roles of miRNAs in osteoblast mineralization.

Key Words
miRNA, FIAT, Sp7, Osteoblast, Regulatory loop.

Introduction

MicroRNAs (miRNAs) are small, functional, highly conserved, noncoding RNAs of 19 to 23 nucleotides that regulate the transcription of mRNAs[1,2]. MiRNAs negatively regulate translation of specific mRNAs by base pairing with partially or fully complementary sequences in target mRNAs to modulate diverse biological and cellular processes[3,4].

Recent studies have suggested that miRNAs played crucial roles in osteoblast differentiation[5]. Nakamura et al[6] confirmed that microRNA-140 regulates endochondral bone development via targeting Dnpep to modulate bone morphogenetic protein (BMP) signaling. Mann et al[7] found that miR-155 inhibits osteogenesis by downregulation of microphthalmia-associated transcription factor (MITF). miR-23a~27a~24-2 cluster was verified to regulate the osteoblast differentiation program through a network connecting RUNX2 and special AT-rich sequence binding protein 2 (SATB2)[8]. Two new miRNAs (miR-2861/miR-3960 cluster) in mouse osteoblasts were identified in our previous studies. We found also that they promoted osteoblast differentiation by repressing histone deacetylase 5 (HDAC5) and homeobox A2 (HOXA2) expression at the post-transcriptional level[9,10]. However, given the great deal of miRNAs, we still need to study the function way of miRNA in osteoblast differentiation.

Matrix mineralization is a key stage in bone formation which is a tightly regulated process. Bone-specific genes and signaling pathways are involved in the regulation of osteoblast mineralization[11,12]. Primary osteoblasts are able to form mineralized nodules in the process of terminal osteoblast differentiation[13]. The present study aimed at investigating the role of target miRNA in the process of osteoblast mineralization *in vitro*.

Materials and Methods

Cell Cultures

Primary mouse osteoblasts were established from calvaria of C57BL/6 mice as previously described[14]. Mouse calvarial osteoblast cultures were grown in a-minimum essential medium (α-MEM, Invitrogen, Carlsbad, CA, USA) supplemented with 5% fetal bovine serum (FBS, Gibco, Rockville, MD, USA), 100 units/mL penicillin, and 100 μg/mL streptomycin. For the

Corresponding Author: Xin-Lan Zhao, MD; e-mail: 244652700@qq.com

induction of mineralization, osteoblasts were cultured in mineralization-inducing medium, α-MEM supplemented with 50 mg/L ascorbic acid (Invitrogen, Carlsbad, CA, USA) and 10 mM β-glycerophosphate (β-GP) (Sigma-Aldrich Chemical Corp., St. Louis, MO, USA) for 21 days in a humidified 5% CO_2 atmosphere at 37°C. The culture medium was changed every 2 days.

Quantitative Reverse Transcriptase-Polymerase Chain Reaction (qRT-PCR) Analysis

Quantitative reverse transcriptase PCR (qRT-PCR) for mRNA or miRNA was performed as previously described using a Roche LightCycler® (Roche Applied Science, Mannheim, Germany)[15]. Total RNA from cultured cells was isolated using TRIzol reagent (Invitrogen, Carlsbad, CA, USA). qRT-PCR was performed using primers for miR-98 or FIAT. Primers were synthesized by PE Applied Biosystems (Norwalk, CT, USA). Amplification data were analyzed using the Sequence Detector System Software (Applied Biosystems, Foster City, CA, USA). Relative quantification was calculated by normalizing the crossing threshold (Ct) values of the test samples with that of the amplified glyceraldehyde 3-phosphate dehydrogenase (GAPDH) or U6 control.

Northern Blot

Northern blotting was performed as described previously[16]. 20 μg of RNA was separated on a 15% polyacrylamide gel in 0.5×Tris borate-EDTA (Ethylene Diamine Tetraacetic Acid, Thermo Fisher Scientific, Waltham, MA, USA) and transferred to a Hybond-N+ nylon membrane (Amersham Pharmacia Biotech, Tokyo, Japan) using a semidry transfer cell (Bio-Rad Laboratories, Inc., Hercules, CA, USA). Hybridization was executed according to the manufacturer's instructions. Digoxin-Labeled oligonucleotide probes complementary to the mature miR-98 were used in the hybridization. The probes for miR-98 and U6 were 5'-GAATAATATAACTTACTACCTCA-3' and 5'-ATATGGAACGCTTCACGAATT-3', respectively.

Western Blotting

Protein (100 μg) from each sample was loaded into a 7.5% polyacrylamide gel. After electrophoresis, the sodium dodecyl sulphate-polyacrylamide gel electrophoresis (SDS-PAGE) separated proteins were transferred to a polyvinylidene difluoride (PVDF) membrane (Millipore, Billerica, MA, USA). The membrane was blocked with 5% nonfat milk in phosphate buffered saline (PBS) and then incubated with antibodies against FIAT, MAD homolog 7 (SMAD7), and Eph receptor A4 (EPHA4) (Santa Cruz Biotechnology, Santa Cruz, CA, USA), or β-actin (Santa Cruz Biotechnology, Santa Cruz, CA, USA) in PBS for 3 h. The membrane was then reprobed with appropriate secondary antibodies conjugated with horseradish peroxidase for 1 h. Blots were processed using an enhanced chemiluminescence (ECL) kit (Santa Cruz Biotechnology, Santa Cruz, CA, USA) and exposed to film.

Alizarin Red S Staining

Osteoblasts were seeded at a density of 2×10^4 cells/well in 24-well plates and treated with medium containing both ascorbic acid and β-GP for 21 days. Mineralization of calcium deposits was assessed by Alizarin Red S (Sigma-Aldrich, St. Louis, MO, USA) staining which was conducted as previously described[15]. To stain for mineralization, cells were fixed with 70% ethanol, rinsed five times with deionized water, treated 10 min with 40 mM Alizarin red stain at pH 4.2, and then, washed with 1×phosphate buffered saline for 15 min with gentle agitation. The stained matrix was assessed using a Nikon Diaphot inverted microscope and was photographed using a Nikon 35-mm camera (Nikon, Tokyo, Japan). As described by Bodine et al[17], Alizarin Red S staining was released from cell matrix by incubation in cetyl-pyridinium chloride, and the amount of released dye was quantified by spectrophotometry at 540 nm.

Bioinformatics Analysis

TargetScan (http://www.targetscan.org/) was used to predict the target gene of miR-98. TF Search (http://www.cbrc.jp/research/db/TFSEARCH.html) was used to find transcription factors which can combine with the promoter of miR-98.

Lentiviral Transduction

The expression vector for the full-length mouse FIAT was constructed by RT-PCR amplification from mouse mRNA using the sense primer 5'-CGTCTAGAGTCCCCAGCTCGAGGATGG-3' and anti-sense primer 5'-GCCGTGGTACCTTAGTGACTGCCTAACA-3'. The PCR product was digested with XbaI-BamHI. Full-length mouse FIAT was transfected into osteoblasts by lentivirus vector named PAJ- FIAT (Auragene Bioscience Inc., Changsha, China)

expressing the reporter gene green fluorescent protein (GFP). F: 5'-CGTCTAGATGCTGCCGTCACCTCATGG-3' R: 5'-GCCGTGGTACCTTAATCTCTACAGAATT- 3'. An 108-bp genomic sequence of the miR-98 precursor (pre-miR-98) was inserted into the PAJ-U6-CMV-eGFP vector (Auragene bioscience, Changsha, China). The primers were 5'-AATTCGCTGCACATGCTGGGGTGAGGTAGTAAGTTGTATT GTTGTGGGGTAGGGATTTTAGGCCCCAGTAAGAAGATAACTATACAACTTACTACTTTCCTTGGTGTGTGGCATGGAAA-3' (forward) and 5'-GATCCTTCCATGCCACACACCAAGGAAAGTAGTAAGTTGTATAGTTATCTTCTTACTGGGGCCTAAAATCCCTACCCCACAACAATACAACTTACTACCTCACCCCAGCATGTGCAGCG-3' (reverse). The oligos were inserted into the Eco.R1-BamHI site in the vector.

The 3'-UTR of mouse FIAT was amplified from total RNA extracted from osteoblasts by reverse transcription-PCR (RT-PCR) using primers designed according to the 3' UTR regions of the mouse FIAT sequence (F: 5'-GGCTCTAGAGTCACCTCAGCGGCCATTC-3'; R: 5'-GGCCGGCCCCGACAGCCAGTCAAAGA-3') The QuikChange site-directed mutagenesis kit (Stratagene, Santa Clara, CA, USA) was used to generate the two mutations in the binding sites of miR-98 in FIAT (mutant FIAT) (F: 5'-CAGGTGTTGCAGAAAAAAAAATCTAGGTCTTTCAGACTGTAGATGG-3'; R: 5'-CCATCTACAGTCTGAAAGACCTAGATTTTTTTTTCTGCAACACCTG-3') by PCR using the WT FIAT construct as the template. The introduced mutations did not result in amino acid changes in the FIAT protein. Finally, the WT and mutant FIAT were cloned into the pAJ expression vector (Auragene Bioscience, Changsha, China) at XbaI-BamHI (FseI) sites.

Gene silencing was performed by using lentiviral shRNA. A lentiviral shRNA vector, named PAJ-sh-FIAT (Auragene Bioscience, Changsha, China) containing shRNA sequence directed against FIAT was produced by Auragene. The product was digested with Eco.R1-BamHI and subcloned into the vector containing a GFP cassette for checking. The scrambled control (TTCTCCGAACGTGTCACGT) was used as a control named PAJ-sh-C (Auragene Bioscience, Changsha, China).

The virus was packaged in HEK293T (ATCC, Manassas, VA, USA) cells. Transfection experiment was carried out according to the manufacturer's protocols. Osteoblasts were infected with FIAT, pre-miR-98, WT- FIAT, MUT-FIAT, and FIAT shRNA lentiviral particles or their controls at 30% to 40% confluence on day 3 and then cultured in differentiation medium. Lentiviral transduction efficiency was checked by observing GFP expression. Then, osteoblasts were seeded at a density of 2×10^4 cells/well in 24-well plates to assay osteogenic functions of interventions following differentiation for 21 days. The mRNA, protein levels and Alizarin Red S staining were detected on day 5 or 21.

The miRNA inhibitors 2′-O-methyl antisense oligonucleotide targeted toward miR-98 (anti-miR-98) and miRNA inhibitor negative control (anti-miR-C) were purchased from GenePharma Co. (Shanghai, China). For stable transfection of pre-miR-98, cells were transfected with the plasmid construct using Lipofectamine 2000 (Invitrogen, Carlsbad, CA, USA) according to the manufacturer's instructions. Stably transfected cells were selected using puromycin (1 μg/mL). For transient transfection, a complex of Lipofectamine 2000 (Invitrogen, Carlsbad, CA, USA) and plasmids or RNA oligonucleotides were prepared according to the manufacturer's instructions and directly mixed with cells in 24-well cell culture plates at a density of 3×10^4 cells per well.

Luciferase Reporter Assay

Pre-miR-98 was inserted into the BamHI-HindIII site in the pSilencer 4.1-CMV vector (Ambion, Austin, TX, USA). The putative target site of miR-98 was amplified using mouse cDNA as template. The PCR products were inserted into the XbaI-FseI site immediately at the downstream of the stop codon in the pGL3 basic luciferase reporter vector (Promega Corp., Madison, WI, USA).

Full-length mouse SP7 was constructed by RT-PCR amplification (F: 5'-CGTCTAGAGTCCCCAGCTCGAGGATGG-3'. R: 5'-GCCGTGGATCCTTAGTGACTGCCTAACA-3'). Promoter PCR product was subcloned into the pGL3 basic vector (Promega, Madison, WI, USA). A 517 bp DNA fragment of the mouse upstream promoter regions of miR-98 containing the putative target site of Sp7 was PCR-amplified using mouse cDNA as template (F: 5′-GGGCGGGCTCTAAAT-3′ R: 5′-AAACACCCTCCCTGGT-3′). The QuikChange site-directed mutagenesis kit (Strata-gene, La Jolla, CA, USA) was used to introduce mutations into the seed region of WT-pGL3-Sp7 or WT-pGL3-promoter. The primers for miR-98 promoter mutagenesis were: F: 5'-GAAAAGCAGGAAGGACCCTCGCCCTTCAAACCC-3'; R: 5'-GGGTTTGAAGGGCGAGGGTCCTTCCTGCTTTTC-3'. WT-pGL3-Sp7 or WT-pGL3-pro-

moter and MUT-pGL3-Sp7 or MUT-pGL3-promoter used for the luciferase reporter assay were produced as described in a previous study[15].

Osteoblasts were transfected using Lipofectamine 2000 with either the wild-type or mutant pcDNA3.1-Sp7 and pre-miR-98 or miR-C constructs for 48 h. In another group, osteoblasts were transfected using Lipofectamine 2000 with either the wild-type or mutant promoter and full-length Sp7 or control constructs for 48 h. As a positive control, the modified pcDNA3.1 control vector was used without a CDS or full-length Sp7 insert. Cells treated solely with Lipofectamine served as negative controls. Firefly and Renilla luciferase activities were determined using the Dual-Luciferase Reporter Assay System (Promega, Madison, WI, USA) with firefly luciferase activities, which is normalized by Renilla luciferase activities from the cotransfected phRL-null vector.

Electrophoretic Mobility Shift Assay (EMSA)

Preparation of nuclear extracts and EMSA were performed as previously described[15]. For the gel shift assay, double-stranded oligonucleotide probes containing the binding sequence for Sp7 were derived from the miR-98 promoter (wild-type oligo D1 sequence: 5'-CAACTTC-CCCGTCCCAGGAAGGAC-3'. The probe and the complementary strand were annealed and end-labeled with digoxin using T4 polynucleotide kinase according to the manufacturer's protocols (Roche Applied Science, Basel, Switzerland). For competition, the EMSA was performed by adding a 1:10 or 1:100 excess of unlabeled wild-type or mutant oligonucleotide (mutant oligo D1 sequence, 5'-CAACTT CCCCtTatC AGGAAG-GAC-3'. For supershift, antibodies against Sp7 or control antibodies (Santa Cruz Biotechnology, Santa Cruz, CA, USA) were added to the incubation mixture. EMSA was performed using a digoxin gel shift kit following the manufacturer's instructions (Roche Applied Science, Basel, Switzerland).

Chromatin Immunoprecipitation (ChIP)

Cells were grown to 70% confluence and cross-linked with 1% formaldehyde at 37°C in the presence of 4% CO_2 for 15 min. The cells were then lysed, DNA-protein complexes were immunoprecipitated, and the formaldehyde-cross-linked DNA was reverse cross-linked with a ChIP assay kit (Upstate, Charlottesville, VA, USA) according to the manufacturer's protocol. DNA-chromatin complexes were immunoprecipitated with anti-Sp7 (Santa Cruz, Santa Cruz, CA, USA), no antibody, or normal mouse IgG (Santa Cruz Biotechnology, Santa Cruz, CA, USA) as an internal control. The precipitated DNA was analyzed by PCR. The primers used for this analysis were as follows: Primer A (-1746/-1562): F: TGTCAAGTTCTG-GTCGTG R: GGAATAACCGCCTCC; Primer B (-1968/-1769): F: TGGTTCCTAACGGGAGA R: GCTGTGGGAATGTCCC; Primer C (-221/-62): F: GGACCTCTGGACTATTGG R: TAGGGTCATG-GTCTCCC.

Statistical Analysis

All experiments were repeated at least three times, and representative experiments are shown. Statistical Product and Service Solutions (SPSS) 19.0 software (IBM, Armonk, NY, USA) was used for statistical analysis. All quantitative data were expressed as mean ± standard deviation. Comparison between groups was done using One-way ANOVA test followed by Post Hoc Test (Least Significant Difference). p values < 0.05 were considered statistically significant.

Results

MiR-98 Expression Dramatically Up-Regulated During Osteoblast Differentiation

Our previous study[15] found that miR-98 expression was significantly up-regulated during osteoblast mineralization. Osteoblasts were cultured in medium supplemented with 50 mg/L ascorbic acid and 10 mM β-glycerophosphate. In the present study, qRT-PCR analysis was used to prove the miR-98 expression pattern during osteoblast mineralization. Expression of mature miR-98 increased about 8.5 fold from low level on day 3 to high level on day 21 in the process (Figure 1). The results of qRT-PCR showed that miR-98 was significantly up-regulated during ascorbic acid and β-glycerophosphate induced osteoblast mineralization. It indicated that miR-98 probably played a role in osteoblast mineralization.

MiR-98 Regulated Ascorbic Acid + β-Glycerophosphate Induced Osteoblast Mineralization

The role of miR-98 in osteoblast mineralization was determined by overexpressing experiment. Ascorbic acid + β-glycerophosphate was used to induce osteoblast mineralization.

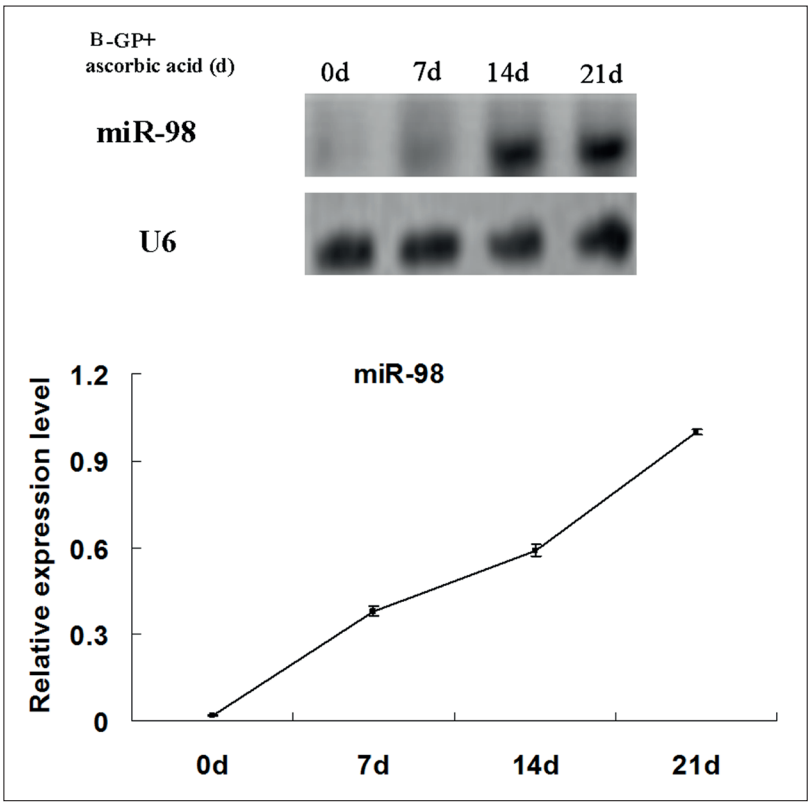

Figure 1. Expression of miR-98 during mineralization of OBs. **A**, Northern blot to verify the expression of miR-98 during mineralization of OBs induced by 50 mg/L ascorbic acid and 10 mM β-glycerophosphate. U6 snRNA was used as loading control (n = 3). **B**, qRT-PCR analysis showed the time-depend ent expression of miR-98 during osteoblasts differentiation and mineralization. Expression of mature miR-98 increased about 8.5 fold from low level on day 3 to high level on day 21 in the process, with a continuous high level during the mineralization process. The level of miR-98 mRNA was normalized to U6 (n = 5). Data were shown as means ± SD.

Osteoblasts were transfected with lentiviral pre-miR-98 on day 3 in the differentiation medium. As a result, after transfection of pre-miR-98 expression vectors, the expression levels of miR-98 was apparently increased compared to empty vector miR-C transfection control (Figure 2A). It indicated that the miR-98 expression vector was constructed successfully and transfection with pre-miR-98 could result in stable overexpression miR-98 in OBs.

Mineralized matrix formation in osteoblasts were evaluated by Alizarin red-S staining after cultured for 14 and 21 days in differentiation medium (Figure 2B). We found that miR-98 overexpression rather than the control reduced the mineralized nodules of osteoblasts. These results indicated that overexpression of miR-98 inhibited mineralization of osteoblasts.

To study the effect of miR-98 on osteoclastogenesis, we constructed miR-98 expression vector by using pre-miR-98. Pre-miR-98 (MI0000586) was the precursor sequence of miR-98 which located in 151913214-151913321 of chromosome X with a length of 107bp and was acquired in the miRBase database.

To detect the effection of miR-98 on the mineralization of osteoblast, we carried out Alizarin red-S staining. Mineralized matrix formation in osteoblasts were evaluated by Alizarin red-S staining after cultured for 14 and 21 days in differentiation medium (Figure 2C). We found that miR-98 overexpression rather than the control increased the mineralized nodules of osteoblasts. These results indicated that overexpression of miR-98 promoted mineralization of osteoblasts.

MiR-98 Directly Targeted Factor Inhibiting Activating Transcription Factor 4 (ATF4)-Mediated Transcription (FIAT)

TargetScan was utilized to analyze and predict the target gene of miR-98. We found a segment in the 3′UTR region of FIAT with well complementarity to miR-98 (Figure 3A) and this sequence was highly conserved among species. Besides, we corroborated TargetScan results with other softwares such as RNA22-HSA (https://cm.jefferson.edu/rna22v1.0-homo_sapiens/). FIAT was reported to play a key role in osteogenesis. It suggested the potential regulatory effect of miR-98 on FIAT gene in osteogenesis. FIAT expression was decreased gradually during osteoblast mineralization (Figure 3B).

To verify that miR-98 functions through binding to the 3'UTR of FIAT mRNA, the 3'UTR fragment containing miR-98 binding site was

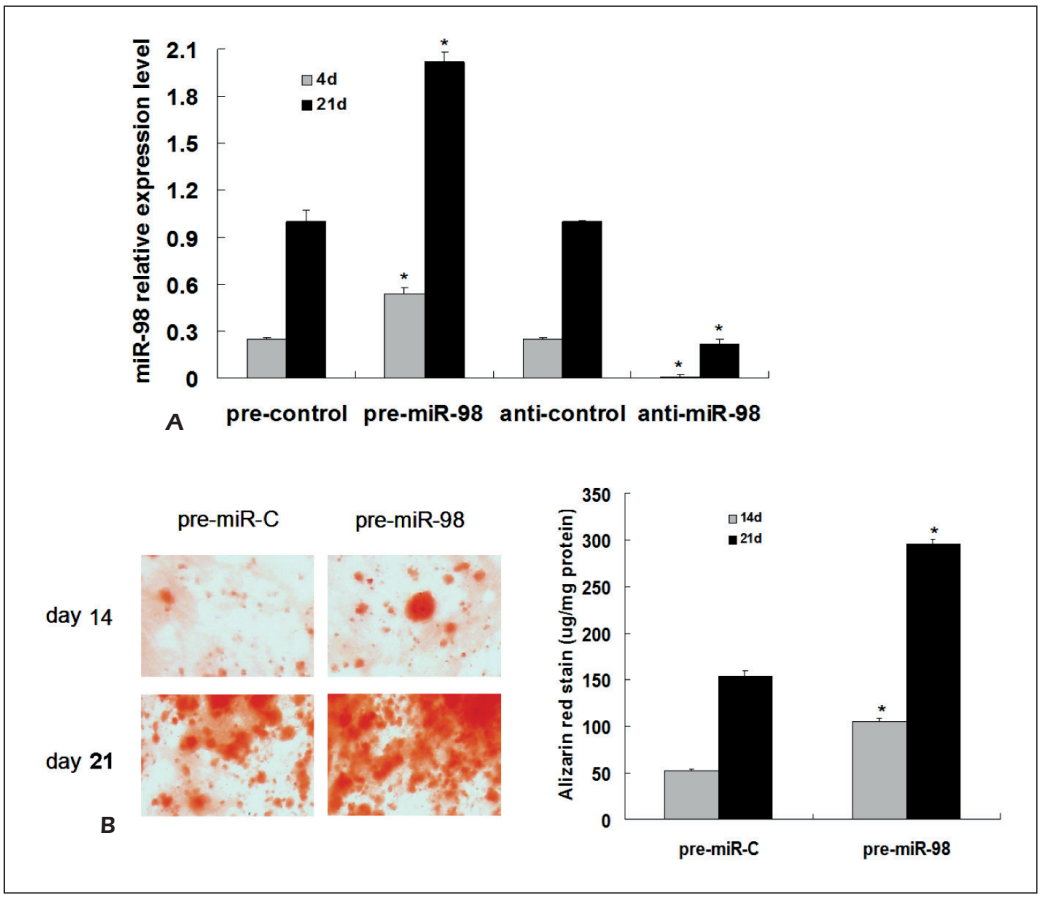

Figure 2. Effects of miR-98 on osteoblast mineralization were shown. **A**, OBs were transfected with pre-miR-98 or anti-miR-98 expression vector. Expression levels of miR-98 in OBs transfected with pre-miR-98 or anti-miR-98 was shown as fold induction relative to β-actin. Expression levels of miR-98 was detected by qRT-PCR. **B**, Microscopic view (left) of effects of miR-98 overexpression on mineralization of the matrix. Osteoblasts infected by lentivirus were cultured in medium with 50 mg/L ascorbic acid and 10 mM β-glycerophosphate for 14 or 21 days. Mineralization of the matrix was determined by Alizarin Red S staining. It was shown a representative microscopic view at a magnification of 200× for control and cells treated with lentivirus infection in cultures of 14 and 21 days. Quantification of Alizarin Red S stains (right) *via* extraction with cetyl-pyridinium chloride. The amount of released dye was quantified by spectrophotometry at 540 nm. The bars represent the mean ± SD (n = 5; *p<0.05 vs. control).

cloned to 3'UTR of dual luciferase reporter gene vector Pgl3 to construct wild-type reporter vector WT-pGL3-FIAT-3'UTR. Either WT-pGL3-FIAT-3'UTR or MUT-pGL3-FIAT-3′UTR was co-transfected into OBs with pre-miR-98 or miR-C, The results showed that, during co-transfection of WT-pGL3-FIAT-3′UTR with miR-98 expression vector, miR-98 bound to 3'UTR of FIAT mRNA so that the luciferase activity was markedly repressed. When the co-transfection system was replaced by miR-C control vector or MUT-pGL3-FIAT-3′UTR, the luciferase activity was not attenuated (Figure 3B). The results validated that miR-98 bound to 3'UTR of FIAT and FIAT was the target gene of miR-98.

Besides, pre-miR-98 was introduced into OBs to identify the function of miR-98 on FIAT directly. Then, ascorbic acid and β-glycerophosphate were treated to induce mineralization of OBs. The results showed that overexpression of miR-98 decreased FIAT protein levels but FIAT mRNA levels was not attenuated (Figure 3C). To evaluate whether miR-98 functions through regulation of other genes than FIAT, which are critical for osteoblast mineralization such as SMAD7 and EPHA4. OBs were transfected with pre-miR-98 or miR-C, and anti-miR-98 or anti-C, the protein levels of SMAD7 and EPHA4 were detected 48h after transfection. The results showed that miR-98 had no affection on SMAD7 and EPHA4. It indicated that miR-98 inhibited FIAT expression at the post-transcriptional level and miR-98 regulated osteoblast mineralization by targeting FIAT.

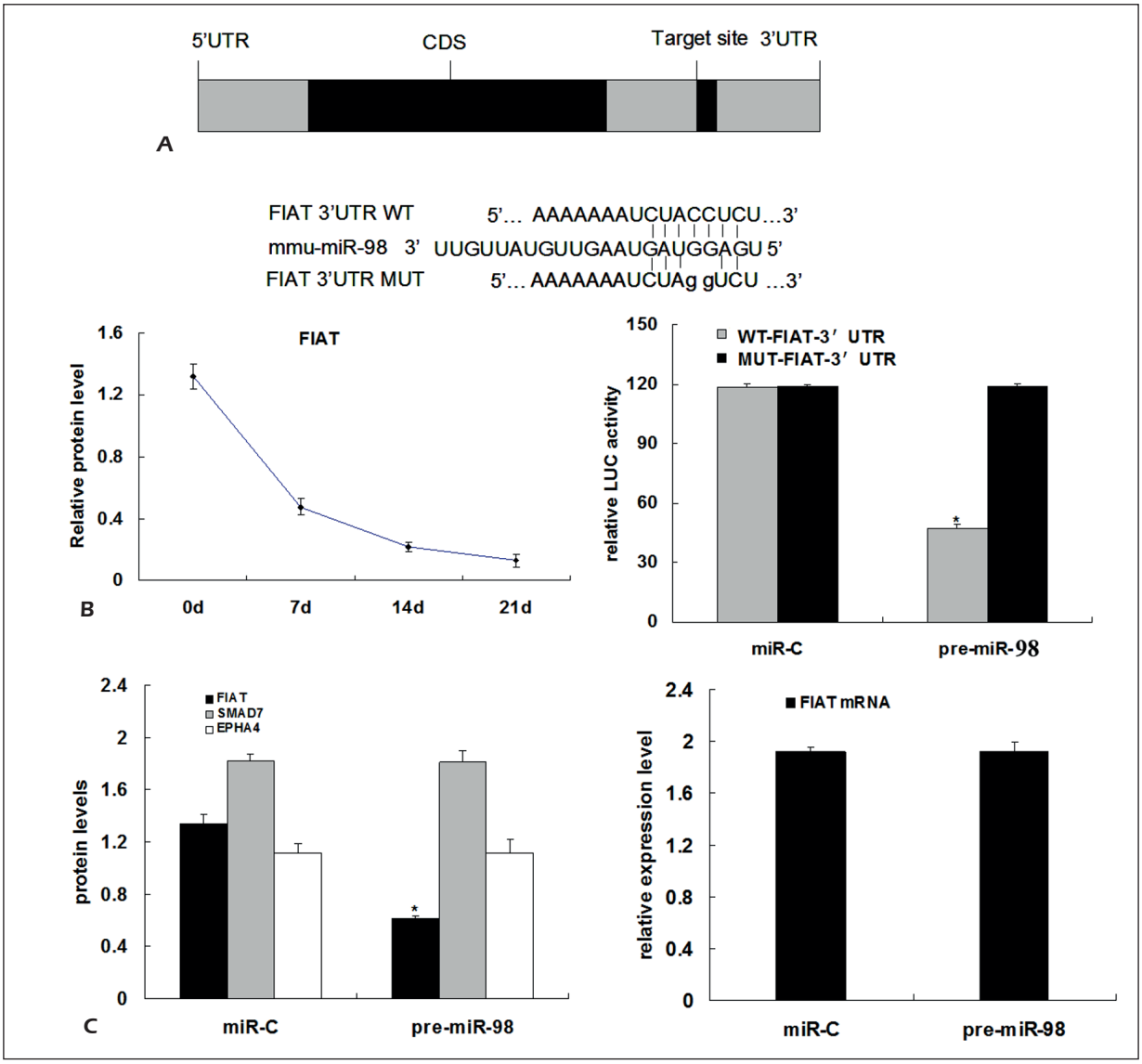

Figure 3. MiR-98 directly targeted FIAT. **A**, Schematic representing the putative target site of miR-98 in mouse FIAT 3'UTR and the base pairing of miR-98 sequences with wild-type (WT) and mutant (MUT) 3'UTR regions of FIAT. Three mutations were underlined. **B**, miR-98 targeted the FIAT 3'UTR. On the left, FIAT expression levels during OB mineralization. FIAT relative protein expression was negatively correlated with miR-98. FIAT expression levels were detected by Western Blot (n=3). On the right, Osteoblasts were cotransfected with the luciferase reporters carrying wild-type FIAT 3'UTR (WT-FIAT-3'UTR) or mutated FIAT 3'UTR (MUT- FIAT-3'UTR) and pre-miR-98 or miR-C for 48 h. The bar chart showed the luciferase activities. Concurrent transfection of pre-miR-98 decreased the reporter activity of WT-FIAT-3'UTR but not the reporter activity of MUT-FIAT-3'UTR. The error bars represented the mean ± SD (*, $p<0.05$ versus MUT-FIAT-3'UTR; n = 5). **C**, miR-98 repressed FIAT expression post-transcriptionally. Osteoblasts were infected by pre-miR-98 or miR-C lentivirus and protein was extracted after culture for 48 hours. On the left, Western blot showed only FIAT protein expression was reduced in the group by miR-98 over-expression. miR-98 overexpression resulted in an about threefold decrease in the amount of FIAT protein. Results were indicated as the ratio of FIAT/β-actin. On the right, Quantitative RT-PCR was used to determine the levels of FIAT mRNA. There is no significant change in FIAT mRNA level in response to miR-98 over-expression. The level of FIAT mRNA was normalized to GAPDH. The error bars represent the mean±SD (*$p<0.05$ vs. miR-C; n=5).

We next cotransfected the WT or mutant FIAT 3′-UTR construct with pre-miR-98 into osteoblasts to determine whether the biological effects of miR-98 could be canceled by the mutant FIAT 3′-UTR construct. Osteoblasts were cotransfected with the WT or mutant FIAT 3′-UTR construct and pre-miR-98 or miR-C. Western blotting showed that the mutant FIAT 3′-UTR construct was able to

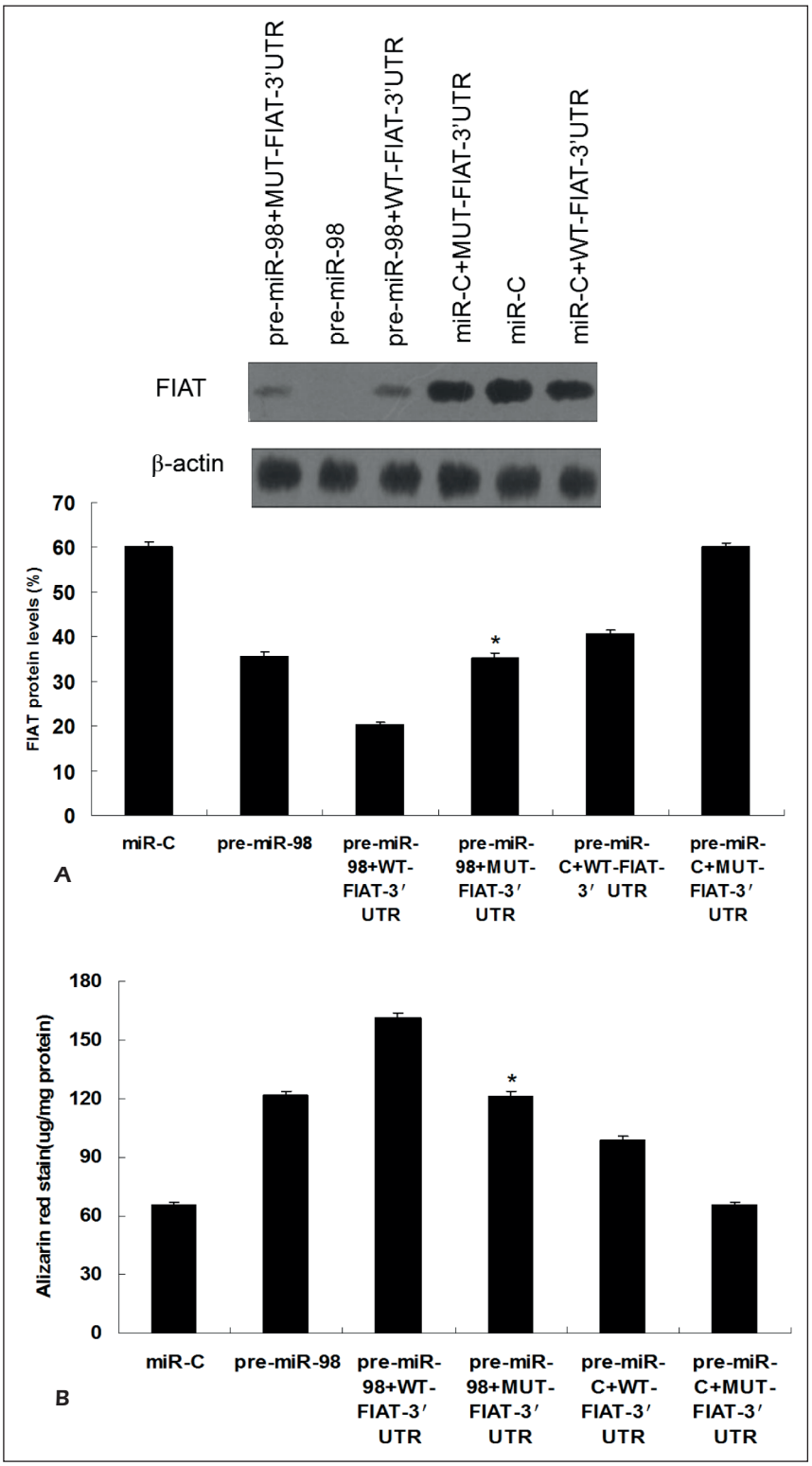

Figure 4. The mutant FIAT-3′UTR construct canceled miR-98-induced promotion of osteoblast mineralization. Osteoblasts were co-transfected with the wild-type (WT) or mutant FIAT-3′UTR construct and pre-miR-98 or miR-C for 21 days. **A**, ransfection of the mutant FIAT-3′UTR into osteoblasts canceled the pre-miR-98-induced downregulation of FIAT protein. **B** , Transfection of mutant FIAT-3′UTR into osteoblasts canceled the pre-miR-98-induced increase of mineralized nodules. Data are shown as means SD (*p<0.05 vs. pre-miR-98+WT-Sp7, n =3).

rescue the pre-miR-98-induced downregulation of FIAT protein (Figure 4A). And results showed that the mutant FIAT 3′-UTR construct was also able to cancel the pre-miR-98-induced promotion of osteoblast mineralization (Figure 4B). This showed that miR-98 regulated osteoblast mineralization by targeting FIAT and fiat was the very important target gene of miR-98 in osteoblast mineralization.

Sp7 Bound to Promoter of miR-98 and Promoted Transcription of miR-98

The primary assembly of miR-98 was in 151913214-151913321 of chromosome X. Recently, Marson et al[18] predicted and validated the promoter and transcription start sites (TSS) for miRNA used the genomic coordinates of the trimethylation of Lys 4 of histone 3 (H3K-4me3)-enriched loci derived from multiple cell types and bioinformatic analysis. The TSS of miR-98 was located in 147143897-147144097 of mouse sapiens chromosome X. We examined 2 kb of the regions upstream of the miR-98 TSS. Using the TF-Search prediction program, we found a potential binding site for Sp7 located 1706-1714 nucleotides upstream from the TSS of the miR-98 (Figure 5A). As our previous study reported[15], Sp7 expression was gradually increased during osteoblast mineralization and reached a peak on day 14.

To verify whether Sp7 bound to the predicted binding site in the promoter of miR-98, EMSA was performed with nuclear protein extracted from ascorbic acid + β-glycerophosphate induced osteoblast mineralization. Double-stranded oligonucleotides containing Sp7 putative binding site were labeled and used as probes. The shift band of wild-type probes and Sp7 complex was formed. The specificity of the binding was confirmed by the competition and supershift assays. An unlabeled wild-type probe competed with the binding complex in a dose-dependent manner. In contrast, a mutant probe had no such competitive effect. To verify the existence of Sp7 in the binding complex, a specific Sp7 antibody was added and a supershift band was then observed, whereas control IgG antibody had no such effect (Figure 5B). To further validate that Sp7 bound to the promoter of miR-98 endogenously in osteoblast, ChIP assay was performed. The cross-linked and fragmented protein-chromatin complexes were immunoprecipitated with Sp7 antibody, no antibody or control IgG antibody. The precipitated DNA was subjected to PCR amplification with specific primers for miR-98 promoter region containing Sp7 binding site. Primer A (-1562--1746) spans the putative binding site of Sp7 in the promoter of miR-98. Primer B and Primer C that span the 5'- and 3'- distal regions of the putative binding site were used as negative controls in the PCR assays. PCR product of miR-98 was obtained from DNA immunoprecipitated with Sp7 antibody, while no PCR product was obtained from DNA immunoprecipitated with control antibody (Figure 5C). These findings provided evidence that Sp7 bound to a putative binding site of the miR-98 promoter.

To verify the link between Sp7 and miR-98 expression, the promoter regions of miR-98 contained the Sp7 binding site or Sp7 binding site mutation (Figure 5D) was cloned into luciferase reporter, and then, cotransfected with full-length Sp7 or empty vector for promoter activity assays. As shown in Figure 5D, compared to control, miR-98 promoter activities were significantly reduced by Sp7 while there was no significant difference in the promoter activities between the Sp7 binding site mutation transfected and control cells (Figure 5D). These data suggested that Sp7 directly promoted expression of miR-98 via physical binding the promoter regions of miR-98.

To further investigate the action of Sp7 on miR-98 transcription, we changed the expression levels of Sp7 in OBs by means of full-length Sp7 or short hairpin RNA (shRNA) against Sp7 lentivirus expression vectors. Empty vector or shRNA control was used as a control. The results showed that overexpression of Sp7 promoted miR-98 transcription, and down-regulation of Sp7 expression caused a decrease in miR-98 transcription in OBs (Figure 5E). These results suggested that Sp7 promoted the transcription of miR-98 by binding to the putative binding site of its promoter.

Discussion

Our study showed that miR-98 regulated osteoblast mineralization through the bone-specific factor FIAT and the expression of miR-98 was regulated by Sp7.

Many miRNAs and factors participated in osteoblast differentiation, proliferation, and mineralization[19]. In our previous report[15], microarray revealed that miR-98 increased greatly during osteoblast mineralization. We then verified that the expression of miR-98 gradually increased during osteoblast mineralization. It suggested that miR-98 played an important role in osteoblast mineralization. The functional role of miR-98 was further confirmed by overexpression experiment. Promotion of mineralization occurred in the miR-98 overexpression group compared with the control. These results indicated that miR-98 regulated osteoblast mineralization, and then our study revealed the mechanism of this action.

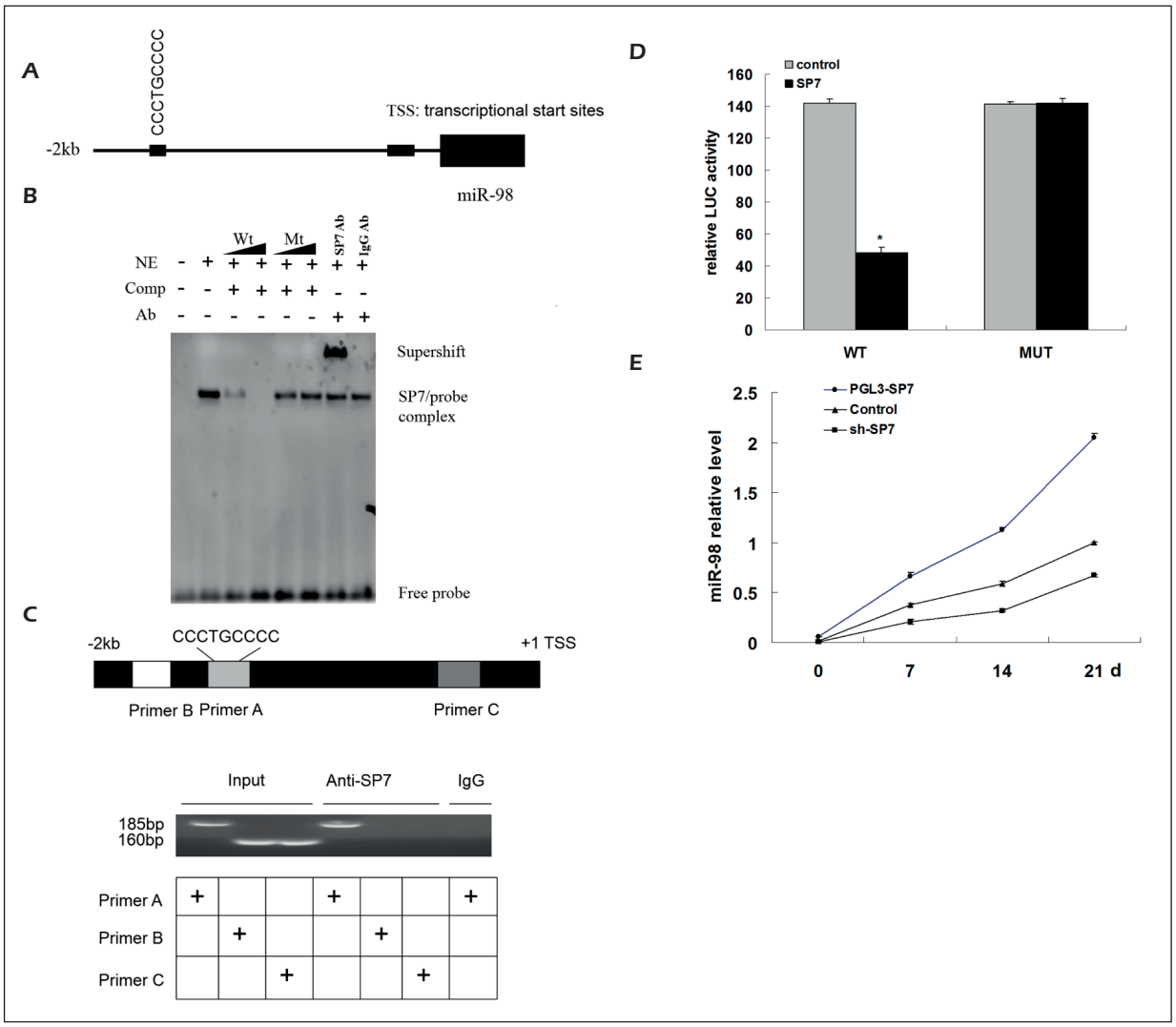

Figure 5. Analysis of Sp7 binding to promoter of miR-98. **A**, A Sp7 binding site was located upstream of miR-98. **B**, EMSA for Sp7 binding to the promoter of the miR-98. Electrophoretic mobility shift assays were performed using labeled oligonucleotide probes derived from the promoter of miR-98 of induced osteoblasts. The labeled oligonucleotide probes (WT Oligo 1) were incubated alone (lane 1), in combination with nuclear extracts (NE; lane 2), in the presence of 10- or 100-fold molar excess of specific unlabeled competitor probe (WT Oligo1) (comp; lanes 3 and 4) or unlabeled mutant (Mt) competitor probe (comp; mutant Oligo 1) (lanes 5 and 6), and in the presence of the Sp7 antibody (anti-Sp7) (Ab; lane 7) or IgG control antibody (Ab; lane 8) (n = 3). **C**, Upper, Schematic representation of the promoter region of miR-98. The positions of the Sp7 binding site and primer sites for ChIP assays are indicated. Lower, ChIP assay showed Sp7 binding to miR-98 through the putative Sp7 binding site. ChIP assays were performed using no-antibodies (input; lanes 1, 2, and 3), Sp7 antibodies (lanes 4, 5, and 6), and control IgG antibody (lane 7). Primer-B (-1968/-1769; lanes 2 and 5) and primer-C (-221/-62, lanes 3 and 6) were used as negative controls for PCR. **D**, Osteoblasts were infected with Sp7 lentivirus (PAJ-Ubi-Sp7), sh-Sp7 lentivirus (PAJ-sh-Sp7) or PAJ-C, shRNA control (sh-C) for 48 h. Sp7 protein levels were elevated or decreased after infection for 48 h. **E**, qRT-PCR 48 hours after Sp7 lentivirus transduction and the 0, 7, 14, and 21 day of Sp7-overexpressing cells showed miR-98 increased and Sp7-knockdown cells showed miR-98 decreased (*, $p<0.05$ vs. miR-C; n=5).

Targetscan was used to predict the target genes related to osteoclast differentiation. TargetScan predicts biological targets of miRNAs by searching for the presence of conserved 8 mer and 7 mer sites that match the seed region of each miRNA. We found that factor inhibiting activating transcription factor 4 (ATF4)-mediated transcription (FIAT), a leucine zipper nuclear protein, was one of the predicted genes by TargetScan. Targetscan provided us one conserved miR-98 target in 3'UTR of FIAT. Furthermore, our data showed that FIAT decreased during osteoblast

mineralization. Meanwhile, the 3′UTR of FIAT harbors a binding site for miR-98, suggesting that FIAT might be a direct target of miR-98. We therefore evaluated the effect of miR-98 on FIAT.

FIAT is a transcription factor playing a crucial role in osteoblast mineralization. It impairs osteoblast activity[20]. FIAT can both modulate early osteoblast activity by interacting with ATF4 and regulate later osteoblast function[21]. FIAT inhibition of matrix mineralization requires dimerization with ATF4 through the second leucine zipper. Furthermore, transgenic mice overexpressing FIAT exhibit osteopenia[22]. Due to this critical regulation of the osteoblast phenotype by FIAT, identifying upstream regulators of this gene is the key to our understanding of osteoblast mineralization.

Our results showed that during osteoblast mineralization the level of miR-98 gradually increased which was reverse to that of FIAT. MiRNAs carry out functions by negatively regulating translation of specific mRNAs[23]. We explored the effects of miR-98 on FIAT. As a result, overexpression of miR-98 only decreased the expression of FIAT protein but not mRNA, which suggested that miR-98 regulates osteoblast mineralization *via* suppressing FIAT in post-transcriptional level.

MiRNAs perform the post-transcriptional inhibition of their target mRNAs mainly by base pairing to the complementary sites in the 3'-UTR of the target mRNA or CDS region of transcription factors[24-26]. The 3'UTR of FIAT harbored a potential target of miR-98 which was predicted by Rna22. The repressive effect of miR-98 on the targeted site of FIAT 3'-UTR was proven by luciferase reporter assay, and mutations of the target site in the FIAT 3'-UTR abolished this repression. It confirmed that FIAT was the targeted mRNA of miR-98.

Marson et al[18] predicted promoter sites and TSS for miRNAs by use of the genomic coordinates of the H3K4me3-enriched loci derived from multiple cell types and bioinformatics analysis. The authors created a library of candidate promoters and TSS for miRNA in both the human and mouse genomes. In the present study, we predicted the promoter and TSS of miR-98 based on these published data.

We then examined the promoter region using the TF-Search prediction program and found a potential binding site (CCCTGCCCC)[27] for Sp7 just upstream of the miR-98 TSS. Sp7 has been demonstrated to be indispensable for the mineralization of osteoblasts *in vivo*[28-31]. In our studies, osteoblasts transfected with Sp7 vector showed increased miR-98 expression level, whereas, block of Sp7 expression inhibited miR-98 transcription. It verified that FIAT acted as an inhibitor of miR-98 expression in osteoblast mineralization. Furthermore, some experiments, such as EMSA, CHIP, and promoter luciferase reporter assay confirmed that Sp7 increased miR-98 expression through binding to the promoter regions of the miR-98. Therefore, we revealed that FIAT protein levels were decreased in osteoblast mineralization *via* the combination between Sp7 and miR-98 promoter, which transcriptionally promoted the expression of miR-98.

These data allowed us to develop a model to demonstrate miR-98-FIAT/Sp7 function loop (Figure 6) which was a part of the complex regulatory network in osteoblast. During the process of osteoblast mineralization, FIAT was a crucial factor that inhibited osteoblast mineralization. Firstly, miR-98 inhibited the expression of FIAT protein, then Sp7 promoted the expression of miR-98. It suggested that there was a unique autoregulatory feedback loop between miR-98, FIAT and Sp7.

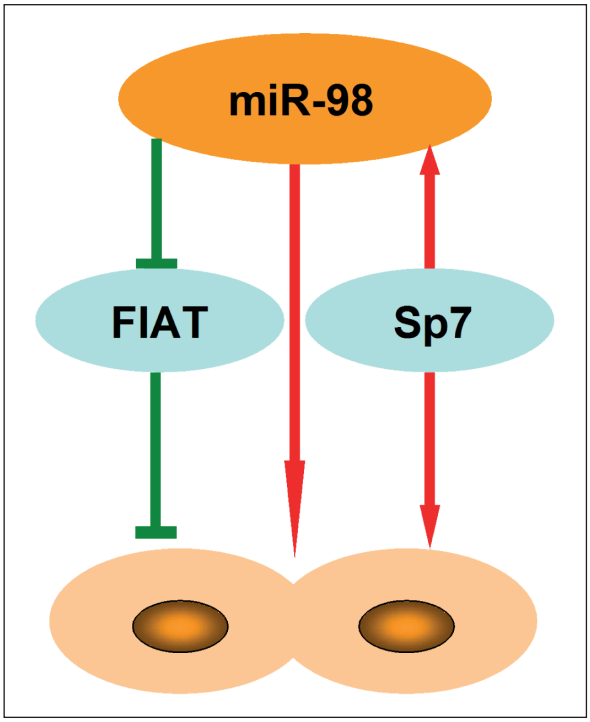

Figure 6. Graphic representation of feedback loop between miR-98, FIAT and Sp7. FIAT was a crucial factor that inhibited osteoblast mineralization. MiR-98 represses the protein levels of FIAT. In turn, Sp7 trans inactivates miR-98. They keep a relative balance in osteoblast mineralization.

Many miRNAs have been identified to mediate osteoblast metabolism. For instance, miR-133 and miR-135 induce osteogenesis of C2C12 mesenchymal cells *via* regulating RUNX2 and SMAD5, respectively[32]. miR-26a negatively regulates osteoblast differentiation by targeting the SMAD1 transcription factor[33]. miR-206 regulated osteoblast differentiation by targeting Cx43[34]. MiR-98, FIAT and Sp7 worked along with those regulatory factors, and played its role in osteoblast differentiation and mineralization.

Conclusions

Our investigation provided evidence that the miR-98 plays an important role in osteoblast mineralization through a novel miR-98-FIAT/Sp7 regulatory feedback loop. Our findings also provide new insights into the roles and regulatory mechanisms of miRNAs in osteoblast mineralization.

Funding Acknowledgements

This work was supported by National Natural Science Foundation grant 81500686 from China and Hunan Provincial Natural Science Foundation grant 2017JJ2154 from China.

Conflict of Interest:

All authors state that they have no conflicts of interest.

References

1) Croset M, Santini D, Iuliani M, Fioramonti M, Zoccoli A, Vincenzi B, Tonini G, Pantano F. MicroRNAs and bone metastasis: a new challenge. Molecules 2014; 19: 10115-10128.
2) Lisse TS, Adams JS, Hewison M. Vitamin D and microRNAs in bone. Crit Rev Eukaryot Gene Expr 2013; 23: 195-214.
3) Thomson DW, Bracken CP, Goodall GJ. Experimental strategies for microRNA target identification. Nucleic Acids Res 2011; 39: 6845-6853.
4) Helwak A, Kudla G, Dudnakova T, Tollervey D. Mapping the human miRNA interactome by CLASH reveals frequent noncanonical binding. Cell 2013; 153: 654-665.
5) Li JP, Zhuang HT, Xin MY, Zhou YL. MiR-214 inhibits human mesenchymal stem cells differentiating into osteoblasts through targeting beta-catenin. Eur Rev Med Pharmacol Sci 2017; 21: 4777-4783.
6) Nakamura Y, Inloes JB, Katagiri T, Kobayashi T. Chondrocyte-specific microRNA-140 regulates endochondral bone development and targets Dnpep to modulate bone morphogenetic protein signaling. Mol Cell Biol 2011; 31: 3019-3028.
7) Mann M, Barad O, Agami R, Geiger B, Hornstein E. MiRNA-based mechanism for the commitment of multipotent progenitors to a single cellular fate. Proc Natl Acad Sci U S A 2010; 107: 15804-15809.
8) Hassan MQ, Gordon JA, Beloti MM, Croce CM, van Wijnen AJ, Stein JL, Stein GS, Lian JB. A network connecting Runx2, SATB2, and the miR-23a~27a~24-2 cluster regulates the osteoblast differentiation program. Proc Natl Acad Sci U S A 2010; 107: 19879-19884.
9) Li H, Xie H, Liu W, Hu R, Huang B, Tan YF, Xu K, Sheng ZF, Zhou HD, Wu XP, Luo XH. A novel microRNA targeting HDAC5 regulates osteoblast differentiation in mice and contributes to primary osteoporosis in humans. J Clin Invest 2009; 119: 3666-3677.
10) Hu R, Liu W, Li H, Yang L, Chen C, Xia ZY, Guo LJ, Xie H, Zhou HD, Wu XP, Luo XH. A Runx2/miR-3960/miR-2861 regulatory feedback loop during mouse osteoblast differentiation. J Biol Chem 2011; 286: 12328-12339.
11) Hughes-Fulford M, Li CF. The role of FGF-2 and BMP-2 in regulation of gene induction, cell proliferation and mineralization. J Orthop Surg Res 2011; 6: 8.
12) Phimphilai M, Zhao Z, Boules H, Roca H, Franceschi RT. BMP signaling is required for RUNX2-dependent induction of the osteoblast phenotype. J Bone Miner Res 2006; 21: 637-646.
13) Bellows CG, Aubin JE, Heersche JN, Antosz ME. Mineralized bone nodules formed in vitro from enzymatically released rat calvaria cell populations. Calcif Tissue Int 1986; 38: 143-154.
14) Owen TA, Aronow M, Shalhoub V, Barone LM, Wilming L, Tassinari MS, Kennedy MB, Pockwinse S, Lian JB, Stein GS. Progressive development of the rat osteoblast phenotype in vitro: reciprocal relationships in expression of genes associated with osteoblast proliferation and differentiation during formation of the bone extracellular matrix. J Cell Physiol 1990; 143: 420-430.
15) Yang L, Cheng P, Chen C, He HB, Xie GQ, Zhou HD, Xie H, Wu XP, Luo XH. MiR-93/Sp7 function loop mediates osteoblast mineralization. J Bone Miner Res 2012; 27: 1598-1606.
16) Gao F, Nan F, Feng J, Lv J, Liu Q, Xie S. Identification and characterization of microRNAs in Eucheuma denticulatum by high-throughput sequencing and bioinformatics analysis. RNA Biol 2016; 13: 343-352.
17) Bodine PV, Trailsmith M, Komm BS. Development and characterization of a conditionally transformed adult human osteoblastic cell line. J Bone Miner Res 1996; 11: 806-819.
18) Marson A, Levine SS, Cole MF, Frampton GM, Brambrink T, Johnstone S, Guenther MG, Johnston WK, Wernig M, Newman J, Calabrese JM, Dennis LM, Volkert TL, Gupta S, Love J, Hannett N, Sharp PA, Bartel DP, Jaenisch R, Young RA. Connecting microRNA genes to the core transcriptional regulatory circuitry of embryonic stem cells. Cell 2008; 134: 521-533.

19) Taipaleenmaki H, Bjerre HL, Chen L, Kauppinen S, Kassem M. Mechanisms in endocrinology: micro-RNAs: targets for enhancing osteoblast differentiation and bone formation. Eur J Endocrinol 2012; 166: 359-371.
20) St-Arnaud R, Mandic V. FIAT control of osteoblast activity. J Cell Biochem 2010; 109: 453-459.
21) St-Arnaud R, Mandic V, Elchaarani B. FIAT, the factor-inhibiting ATF4-mediated transcription, also represses the transcriptional activity of the bZIP factor FRA-1. Ann N Y Acad Sci 2010; 1192: 338-343.
22) Yu VW, El-Hoss J, St-Arnaud R. FIAT inhibition increases osteoblast activity by modulating Atf4-dependent functions. J Cell Biochem 2009; 106: 186-192.
23) Van Wynsberghe PM, Chan SP, Slack FJ, Pasquinelli AE. Analysis of microRNA expression and function. Methods Cell Biol 2011; 106: 219-252.
24) Thomson DW, Bracken CP, Goodall GJ. Experimental strategies for microRNA target identification. Nucleic Acids Res 2011; 39: 6845-6853.
25) Tay Y, Zhang J, Thomson AM, Lim B, Rigoutsos I. MicroRNAs to Nanog, Oct4 and Sox2 coding regions modulate embryonic stem cell differentiation. Nature 2008; 455: 1124-1128.
26) Ko HY, Lee DS, Kim S. Noninvasive imaging of microRNA124a-mediated repression of the chromosome 14 ORF 24 gene during neurogenesis. FEBS J 2009; 276: 4854-4865.
27) Wu YF, Matsuo N, Sumiyoshi H, Yoshioka H. Sp7/Osterix is involved in the up-regulation of the mouse pro-alpha1(V) collagen gene (Col5a1) in osteoblastic cells. Matrix Biol 2010; 29: 701-706.
28) Zhou X, Zhang Z, Feng JQ, Dusevich VM, Sinha K, Zhang H, Darnay BG, de Crombrugghe B. Multiple functions of Osterix are required for bone growth and homeostasis in postnatal mice. Proc Natl Acad Sci U S A 2010; 107: 12919-12924.
29) Yang F, Tang W, So S, de Crombrugghe B, Zhang C. Sclerostin is a direct target of osteoblast-specific transcription factor osterix. Biochem Biophys Res Commun 2010; 400: 684-688.
30) Zhang C. Transcriptional regulation of bone formation by the osteoblast-specific transcription factor Osx. J Orthop Surg Res 2010; 5: 37.
31) Nakashima K, Zhou X, Kunkel G, Zhang Z, Deng JM, Behringer RR, de Crombrugghe B. The novel zinc finger-containing transcription factor osterix is required for osteoblast differentiation and bone formation. Cell 2002; 108: 17-29.
32) Li Z, Hassan MQ, Volinia S, van Wijnen AJ, Stein JL, Croce CM, Lian JB, Stein GS. A microRNA signature for a BMP2-induced osteoblast lineage commitment program. Proc Natl Acad Sci U S A 2008; 105: 13906-13911.
33) Luzi E, Marini F, Sala SC, Tognarini I, Galli G, Brandi ML. Osteogenic differentiation of human adipose tissue-derived stem cells is modulated by the miR-26a targeting of the SMAD1 transcription factor. J Bone Miner Res 2008; 23: 287-295.
34) Inose H, Ochi H, Kimura A, Fujita K, Xu R, Sato S, Iwasaki M, Sunamura S, Takeuchi Y, Fukumoto S, Saito K, Nakamura T, Siomi H, Ito H, Arai Y, Shinomiya K, Takeda S. A microRNA regulatory mechanism of osteoblast differentiation. Proc Natl Acad Sci U S A 2009; 106: 20794-20799.